

Computational modelling of TRIANGULAR sub-boundary-layer vortex generators

Unai Fernandez-Gamiz^{1*}, Jon Ruiz de Loizaga¹, Iñigo Errasti¹, Ana Boyano², Ekaitz Zulueta³ and Jose Manuel Lopez-Guede³

¹Nuclear Engineering and Fluid Mechanics Dep., University of the Basque Country, Nieves Cano 12, 01006 Vitoria-Gasteiz, Araba, Spain

²Department of Mechanical Engineering, University of the Basque Country (UPV/EHU), Nieves Cano, 12, 01006 Vitoria-Gasteiz, Spain

³Automatic control and System Engineering Dep., University of the Basque Country, Nieves Cano 12, 01006 Vitoria-Gasteiz, Araba, Spain

Abstract. Vortex generators (VGs) are used increasingly more by the wind turbine manufacture industry as flow control devices to improve rotor blade aerodynamic performance. The VG height is usually designed with equal thickness of the local boundary layer at the VG position. Nevertheless, these conventional VGs may produce excess residual drag in some applications. The so-called sub boundary layer VGs can provide enough momentum transfer over a region several times their own height for effective flow-separation control with much lower drag. The main objective is to investigate how well the simulations can reproduce the physics of the flow of the primary vortex generated by a triangular VG mounted on a flat plate with negligible pressure gradient with the angle of attack of the vane to the oncoming flow $\beta = 18^\circ$. Three different device heights $H = 5\text{mm}$, $H_1 = 6,25\text{mm}$, $H_2 = 4,16\text{mm}$ have been studied and compared both qualitatively and quantitatively. To that end, computational simulations have been carried out using RANS method and at Reynolds number $Re = 2600$ based on the boundary layer momentum thickness $\theta = 2.4\text{ mm}$ at the VG position. The computational results show good agreement with the experimental data available in AVATAR project.

1 Introduction

Current wind turbine design is revolving around the 6 to 7 MW capacity range, with increasingly large rotor diameters. These large blades, usually pitch regulated, often have a poor aerodynamic performance near the root due to form and operation limitations, such as the required structural twist of the rotor blades or the relatively thick root sections that are needed in order to transmit the very large bending moments generated at the outer parts of the blade. The fact that root section airfoils are thick is aerodynamically unfavorable because they stall much earlier than thinner airfoils in the mid-outer regions of the blade.

Then, the most relevant aerodynamic problem that arises is boundary layer separation on blades suction side, which causes the rotor to become unstable due to entering stall and brings an important energy loss in this region. In addition, surface roughness and leading edge erosion can also induce local flow separation over time. Consequently, research on boundary layer separation control has gained in

significance in the field of fluid mechanics and different flow control devices have been investigated by authors such as [1,2].

The effect of VGs in a 1 MW and a 2.5 MW wind turbines was investigated by Øye [3] and Sullivan [4], respectively, and a comparison between the measured power curve on a wind turbine with and without VGs was drawn. Results proved that VGs can successfully increase the power production of a wind turbine for nearly all wind speeds. In the work of Fernandez-Gamiz et al. [5], BEM-based computations were carried out on the National Renewable Energy Laboratory (NREL) 5 MW baseline wind turbine with and without flow control devices. The results obtained from the clean wind turbine without any device for flow controlling were compared with the ones obtained from the wind turbine equipped with vortex generators and Gurney flaps. A best configuration case is proposed which has the largest increase of the average power output. In that case, increments on the average power output of 10.4% and 3.5% have been found at two different wind speed realizations

A Vortex Generator (VG) is a passive flow control device which modifies the airflow over the boundary layer

* Corresponding author: unai.fernandez@ehu.eus

via bringing momentum from the outer region into the near wall region. The main consequence of installing Vortex Generators is that the momentum of the near wall region is increased at the same time as the boundary layer thickness is decreased, which in turn results in a delay of the flow separation, Rao et al. [6]. The VG operating principle is based on generating streamwise vortices, see Velte et al. [7,8].

Research on Vortex Generators mounted on a flat plate has previously occupied several researchers, Lin [9] and Martinez-Filgueira et al. [10]. Further research on the control of laminar separation bubbles by means of VGs at moderate Reynolds number was carried out by Kerho et al. [17], showing a significant drag reduction. In addition, Lin et al. [18] reached the conclusion that with the help of VGs of a lower height than the local boundary layer thickness, lift force effect was increased and drag force effect was reduced. Wendt et al. [11] experimentally tested an array of VGs deliberately arranged in order to generate counter rotating vortices. Vortex Generators are usually placed on wind turbine blades with the purpose of delaying local flow separation, thus counterbalancing the negative aerodynamic effects of blades surface roughness. An overview of different airfoils with several VG options is listed in van Rooij and Timmer [5]. According to Schubauer et al. [20] and Bragg et al. [21], VGs represent a cost-effective and practical solution to improving the aerodynamic performance of a wind turbine blade. Fernandez-Gamiz et al. [12,13] and Urkiola et al. [14] studied the behaviour of a rectangular VG on a flat plane and the streamwise vortices produced by them to investigate how the physics of the wake behind VGs in a negligible streamwise pressure gradient flow can be reproduced in CFD simulations and their accuracy in comparison with experimental observations.

The main objective of this work is to carry out a parametric study of a single triangular Vortex Generator mounted on a plate with the purpose of assessing the induced flow effects. For this, Computational Fluid Dynamics (CFD) simulations have been run with two purposes. Firstly, to validate the CFD model VG with specific experimental data and secondly, to study the variation of the main vortex parameters with the VG height. Consequently, three VG heights have been considered for the same computational domain topology of a fully meshed CFD Vortex Generator model: h1=4.16 mm, h2=5 mm and h3=6.25 mm.

2 Baseline Experimental Data

The current study is based on Advanced Aerodynamic Tools of Large Rotors AVATAR European project and the parameters used for the validation of the computational results are the Streamwise velocity profiles at different locations and velocity fields at streamwise planes 10H, 25H and 50H (AVATAR Task 3.1 [15]). Taken into account the previous configuration and in order to characterize the

primary vortex generated by the three different VGs, the streamwise velocity profiles at different downstream locations has been studied.

According to the experimental data available in the AVATAR project and to reproduce the experiments of the VG on a flat plate performed in that project, the numerical simulations have been carried out at a Reynolds number $Re = 2600$ based on local boundary layer BL momentum thickness $\theta = 2.4$ mm and with a free stream velocity of $U_\infty = 15$ m/s. A negligible pressure gradient on the plate is assumed. The angle of incident of the vane to the oncoming flow is 18° . The calculation of the local BL momentum thickness θ was made by the application of eq(1).

$$= \int_0^\infty \frac{u_x}{U_\infty} \left(1 - \frac{u_x}{U_\infty}\right) dy \quad (1)$$

where u_x is the streamwise velocity component, U_∞ the free stream velocity and y de vertical coordinate normal to the wall.

In order to validate the numerical model of the VG, the results of the numerical simulations are compared to the experimental data of AVATAR Project.[15,16]. The experiments were carried out in the Boundary Layer Wind Tunnel of the TU Delft was used for this study. Vortex generator dimensions were designed according to the previous research made by Baldacchino et al.[17], where the triangular vortex generators were designed according to the study of Godard et al. [18] and are summarized in Table 1.

Table 1. Vortex Generator Geometry in the AVATAR project.

VG property	Symbol	Value (mm)	Size (h units)
VG height	H	5.0	1
Vane length	L	12.5	2.5
Distance between VG pairs	D	30	6
Trailing edge separation	d	12.5	2.5
Incident angle	β	18°	-
Local boundary layer thickness	δ	20	4

3 Computational Setup

The computational domain is divided in 28 blocks. The mesh has been refined near the VG and in the corners of the vane where the velocity gradients are large. In regions far away the VG and the wake, the mesh density is lower. Five blocks are located around the VG and six blocks downstream of the vane to capture the generated primary vortex. It has been followed the same block based meshing strategy as in the study of Urkiola et al. [14]. The total amount of cells is 8 million, with a height of the first cell of $\Delta y/H = 3.23 \times 10^{-6}$, normalized according the baseline VG height. Around the vane, the mesh has 1.7

million cells, while the mesh downstream the VG for capturing the wake has approximately 2.4 million cells; see Figure 1. In order to resolve the boundary layer, cell clustering has been used close to the wall and the wall dimensionless distance of the first layer of cells is less than $y^+ < 1$.

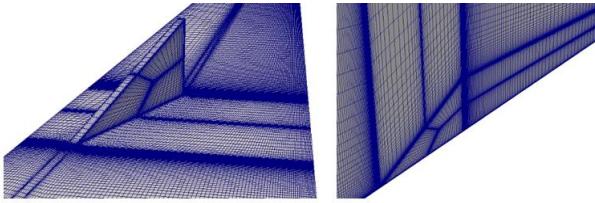


Fig. 1. Mesh refined regions around the VG.

In the present work, the open source code OpenFOAM [19] has been used for simulating a triangular VG on a flat plate with negligible pressure gradient. This CFD code is an object-oriented library written in C++ to solve computational continuum mechanics problems. The simpleFoam solver has been applied for steady-state, incompressible and turbulent flows using the RANS (Reynolds Average Navier-Stokes) equations. Second order discretisation schemes were employed in the CFD simulations. The k- ω SST (Shear Stress Transport) turbulence model developed by Menter [20] was used for all the computations. A mesh independency study has been done with the boundary layer velocity profile at the plane 10H downstream of the VG and at $z=0$ cross-wise position. Figure 2(a) shows a comparison between the CFD curves of three studied meshes: 2 million (coarse), 4 million (medium) and 8 million (fine) cells for the baseline case with a VG height of $H=5$ mm. Figure 2(b) represents the BL velocity profiles of the fine mesh (blue) versus the experimental one (black) provided by [15].

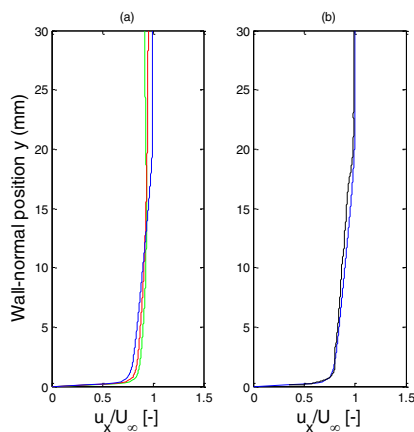


Fig. 2. Comparison of the normalized streamwise velocity profile at 10H downstream plane position and spanwise position of $z=0$ corresponding to the baseline case of $H=5$ mm. (a) CFD curves for three different meshes: coarse (green), medium (red) and fine (blue). (b) BL velocity profiles of the fine mesh (blue) versus the experimental one (black).

4 Results and discussion

In Figure 3, a streamwise velocity profiles comparison between experimental curves provided by TU Delft in AVATAR project and CFD curves for the streamwise planes at $x=5H$ and $x=10H$ and the spanwise planes at $z=0$, $z=+D/5$ ($z/D=+0.2$) and $z=+D/2$ ($z/D=+0.5$) can be seen. In general all CFD and experimental curves correlations are acceptable; however, it is clear that the quality of correlation improves as the distance from the VG in the wake increases.

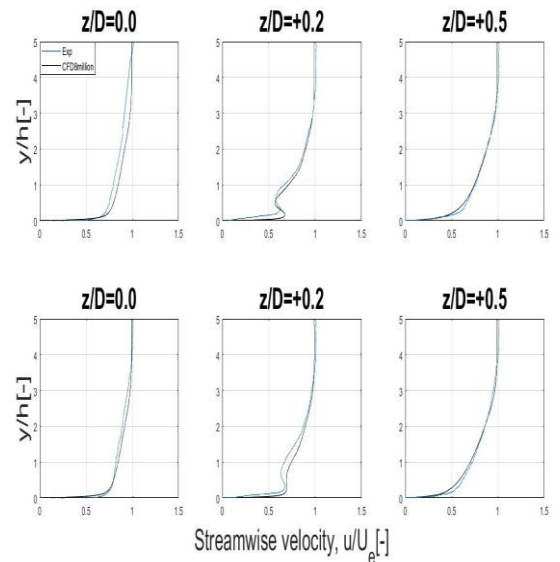


Fig. 3. Comparison of the streamwise (out-of-plane) velocity between experimental and numerical predictions and mesh dependency study. Streamwise station from top to bottom: 5h, 10h.

Figure 4 shows the streamwise velocity profiles comparison between the three VG heights (4.16mm, 5mm and 6.25mm) for the streamwise planes at $x=5H$ and $x=10H$ and the spanwise planes at $z=0$, $z=+D/5$ ($z/D=+0.2$) and $z=+D/2$ ($z/D=+0.5$) can be seen.

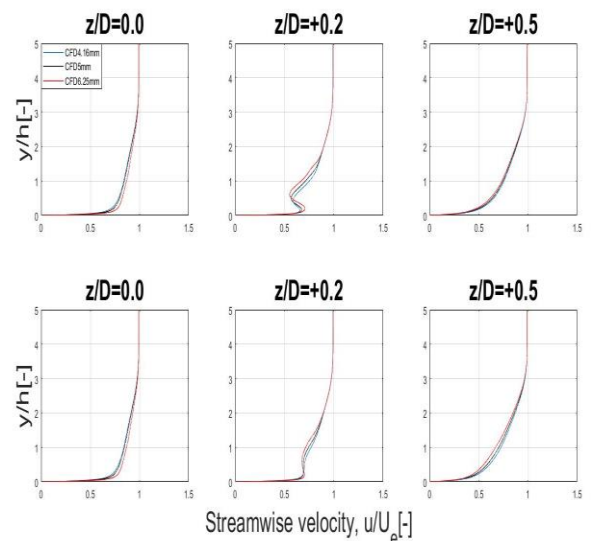


Fig. 4. Comparison of the streamwise (out-of-plane) velocity between the three VG heights. Streamwise station from top to bottom: 5h,10h.

In Figure 5, a velocity field comparison between the three VG heights (4.16 mm, 5mm and 6.25 mm) for the streamwise planes at $x=5H$, $x=10H$, $x=25H$ and $x=50H$ is shown.

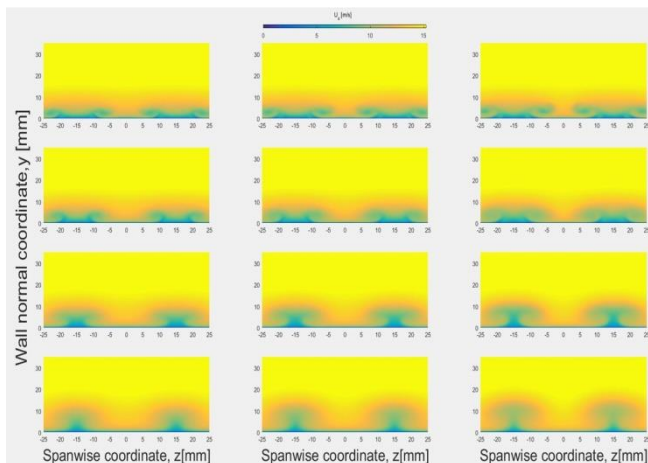


Fig. 5. Contours of out-of-plane velocity u_x .

According to Figure 5, vortex size increases with the distance from the VG trailing edge while the distance between vortex centers decreases. On the other hand, velocity in the middle region of each vortex increases and velocity in the top region decreases with the VG height as a consequence of having a higher vortex center. Moreover, the streamwise planes that show the biggest differences in both middle and top vortex regions with respect to the VG height are the ones at $x=25H$ and $x=50H$.

5 Conclusions

In general, the CFD results obtained in the current work are in concordance with the fact that a pair of higher VGs induce a higher, narrower and more powerful pair of vortices and thus they offer a greater contribution to delaying boundary layer separation.

The development of the induced vortices is such that at the nearest streamwise position, $5H$, their cores are at the lowest position and more separate from each other, whereas at the last streamwise position, $50H$, their cores are at the highest position and collapse into each other as if they were a single vortex. This implies that velocity decreases with the distance from the trailing edge of the VG in between the pair of vortices. In addition, velocity slightly increases and decreases with the VG height in the middle and top vortex regions of each vortex respectively, as a consequence of a higher vortex center.

ACKNOWLEDGMENTS

The funding from the Government of the Basque Country and the University of the Basque Country UPV/EHU through the SAIOTEK (S-PE11UN112) and EHU12/26 research programs, respectively, is gratefully acknowledged.

References

1. Aramendia, I.; Fernandez-Gamiz, U.; Ramos-Hernanz, J.; Sancho, J.; Lopez-Guede, J.; Zulueta, E. Flow Control Devices for Wind Turbines. In *Energy Harvesting and Energy Efficiency: Technology, Methods, and Applications*; Bizon, N.; Mahdavi Tabatabaei, N.; Blaabjerg, F.; Kurt, E., Eds.; Springer International Publishing: Cham, (2017); pp. 629-655.
2. Aramendia-Iradi, I.; Fernandez-Gamiz, U.; Sancho-Saiz, J.; Zulueta-Guerrero, E. State of the art of active and passive flow control devices for wind turbines. *Dyna* (2016), **91**, 512-516, DOI 10.6036/7807.
3. Øye, S. The ELKRAFT 1 MW Wind Turbine: Results from the Test Program. *European Union Wind Energy Conference - Göteborg, Sweden* (1996), 251-255.
4. Sullivan, T.L. Effect of vortex generators on the power conversion performance and structural dynamic loads of the Mod-2 wind turbine. (1984), *NASA-TM-83680*, *E-2131*, *DOE/NASA/20320-59*, *NAS 1.15:83680*.
5. Fernandez-Gamiz, U.; Zulueta, E.; Boyano, A.; Ansoategui, I.; Uriarte, I. Five Megawatt Wind Turbine Power Output Improvements by Passive Flow Control Devices. *Energies* (2017), **10**, DOI 10.3390/en10060742.
6. Atluri, S.; Rao, V.K.; Dalton, C. A numerical investigation of the near-wake structure in the variable frequency forced oscillation of a circular cylinder. *Journal of Fluids and Structures* (2009), **25**, 229-244, DOI <https://doi.org/10.1016/j.jfluidstructs.2008.06.012>.
7. Velte, C.M.; Hansen, M.O.L.; Okulov, V.L. Helical structure of longitudinal vortices embedded in turbulent wall-bounded flow. *J Fluid Mech* (2009), **619**, 167-177, DOI 10.1017/S0022112008004588. Available

- online:
<http://dx.doi.org/10.1017/S0022112008004588>.
8. Velte, C.M. Vortex generator flow model based on self-similarity. *AIAA J* (2012), **51**, 526-529, DOI 10.2514/1.J051865.
 9. Lin, J. Review of research on low-profile vortex generators to control boundary-layer separation. *Prog Aerospace Sci* (2002), **38**, 389-420, DOI 10.1016/S0376-0421(02)00010-6.
 10. Martínez-Filgueira, P.; Fernandez-Gamiz, U.; Zulueta, E.; Errasti, I.; Fernandez-Gauna, B. Parametric study of low-profile vortex generators. *Int J Hydrogen Energy* (2017), **42**, 17700-17712, DOI <https://doi.org/10.1016/j.ijhydene.2017.03.102>.
 11. Wendt, B. Parametric study of vortices shed from airfoil vortex generators. *AIAA J* (2004), **42**, 2185-2195, DOI 10.2514/1.3672.
 12. Fernandez, U.; Velte, C.M.; Rethore, P.-.; Sorensen, N.N. Self-Similarity and helical symmetry in vortex generator flow simulations. *Science of Making Torque from Wind 2012* (2014), **555**, DOI 10.1088/1742-6596/555/1/012036.
 13. Fernandez-Gamiz, U.; Velte, C.M.; Réthoré, P.; Sørensen, N.N.; Egusquiza, E. Testing of self-similarity and helical symmetry in vortex generator flow simulations. *Wind Energy* (2016), **19**, 1043–1052, DOI 10.1002/we.1882.
 14. Urkiola A., Fernandez-Gamiz U., Errasti I., Zulueta E. Computational characterization of the vortex generated by a vortex generator on a flat plate for different vane angles. *Aerospace Science and Technology* (2017), **65**, 18-25.
 15. Baldacchino D. Experimental data description for avatar task 3.1: experimental investigation of low-profile vortex generators in a boundary layer wind tunnel. January (2015), <http://www.eera-avatar.eu>.
 16. Ferreira, C., Gonzalez, A., Baldacchino, D., Aparicio, M., Gómez, S., Munduate, X., Barlas, A., Garcia N. R., Sorensen, N. N., Troldborg, N., Barakos, G., Jost, E., Knecht, S., Lutz, T., Chassapoyiannis, P., Diakakis, K., Manolesos, M., Voutsinas, S., Prospathopoulos, J., Gillebaart, T., Florentie, L., van Zuijlen, A., Reijerkerk, M. FP7 AVATAR Project Task 3.2 : Development of aerodynamic codes for modelling of flow devices on aerofoils and rotors. (2016), <http://www.eera-avatar.eu>.
 17. Baldacchino, D.; Ragni, D.; van Bussel, C.S.F.G.J. Towards integral boundary layer modelling of vane-type vortex generators. *45th AIAA Fluid Dynamics Conference, Dallas, TX* (2015), 12-18.
 18. Godard, G.; Stanislas, M. Control of a decelerating boundary layer. Part 1: Optimization of passive vortex generators. *Aerospace Science and Technology* (2006), **10**, 181-191, DOI <http://dx.doi.org/10.1016/j.ast.2005.11.007>.
 19. OpenFOAM, <https://www.openfoam.org/>, 2017.
 20. Menter, F.R. 2-Equation Eddy-Viscosity Turbulence Models for Engineering Applications. *AIAA J* (1994), **32**, 1598-1605, DOI 10.2514/3.12149.